Aversive Emotion Activates Orexin Neurons and Induces Tachycardia in Freely Moving Mice

Akira Yamashita
Kagoshima University: Kagoshima Daigaku
Shunpei Moriya
Kagoshima University: Kagoshima Daigaku
Ryusei Nishi
Kagoshima University: Kagoshima Daigaku
Jun Kaminosono
Kagoshima University: Kagoshima Daigaku
Akihiro Yamanaka
Nagoya University: Nagoya Daigaku
Tomoyuki KUWAKI (kuwaki@m3.kufm.kagoshima-u.ac.jp)
Kagoshima Daigaku https://orcid.org/0000-0003-4226-3610

Research

Keywords: aversive emotion, stress, orexin, defense response, fiber photometry

Posted Date: December 1st, 2020

DOI: https://doi.org/10.21203/rs.3.rs-115888/v1

Abstract

Stress affects the sensory and negative emotional components in the brain and causes autonomic responses and aversive emotion. However, the possible roles for the negative emotional component remain largely unclear. The perifornical area of the hypothalamus has been known as the center for the defense response, or fight-or-flight response, which is characterized by a concomitant rise in arterial blood pressure, heart rate, and respiratory frequency. Orexin neurons located in that region are suggested to be a critical population responsible for that response. In this study, we examined the suggestion by recording orexin neuronal activity and heart rate in freely moving mice using an original dual-channel fiber photometry system in vivo. Association analysis between orexin neuronal activity and aversive stress-induced autonomic responses revealed a rapid increase in neuronal activity just prior to changes in heart rate. In addition, we examined whether orexin neurons would be activated by a conditioned neutral sound that was previously associated with aversive stimulus. We show that the negative emotional memory indeed activated orexin neurons and increased heart rate. Our data suggest that orexin neurons are the key component required to receive aversive emotion and link it with an autonomic defense response. Our data also suggest that targeting orexin neurons may enable treatment of psychiatric disorders that result from chronic stress and occur long after the original sensory inputs are gone.

Introduction

Stress is often mistakenly thought of as being purely detrimental. While it is true that excessive stress generally has negative effects that can cause various mental disorders and emotional disturbances[1], responses to acute stress can be beneficial and even indispensable for life because they protect against potential sources of danger. Acute stress induces a rise in blood pressure, heart rate, respiration, and stress-induced analgesia. These autonomic changes are collectively called the defense response and prepare for and support fight-or-flight behavior[2]. We previously found that orexin-producing neurons in the hypothalamus play a crucial role in this defense response because it is severely attenuated in orexin knockout mice[3] and orexin neuron ablated mice[4].

Although orexin neurons are essential to autonomic defense responses induced by stress in general, orexin neuronal activity occurring in response to specific stressors remains unclear. In the past, several technical limitations have prevented us from thoroughly examining these unknowns. First, the use of freely moving animals without anesthesia is necessary because stress responses are unable to occur under anesthesia. Second, the hypothalamus contains many different cell types and targeting only the orexin-producing neurons of interest was difficult. Some researchers have reported on the activity of orexin neurons in awake rats by using traditional electrophysiological methods such as extracellular recording, and then subsequently identifying the neurons that were recorded from with immunohistochemistry[5,6]. However, this is a time-consuming approach and therefore is not realistic to use for studying the possible effects of several kinds of stressors while simultaneously recording autonomic stress responses. In addition, single cell recording techniques create a sampling bias: there are about 2000-3000 orexin neurons in the mouse

brain[7] but the activity of only one or two neurons can be recorded at a time. To overcome these limitations, we set out to develop and improve a fiber photometry system.

A fiber photometry system can track the real-time dynamics of genetically specified neuron populations located deep within the brain of freely moving mice by using a single channel fiber and genetically encoded Ca^{2+} indicators[8-10]. We recently utilized a single channel fiber photometry system and successfully recorded orexin[11,12] and dopamine[13] neural activities using G-CaMP6. More recently, we upgraded the system to operate via dual channels. The dual channel system can detect more sophisticated data by virtue of two-color measurement(s) by using one color for reference. The animal's movement sometimes affects the fluorescent signal intensity so this improvement was essential for the simultaneous recording of neuronal activity and animal behavior. We used mCherry signal as a reference to G-CaMP signal. Although we briefly reported on this dual channel system in our previous paper[12], it will be described in more thorough detail here. The system with dual-channel was previously published independently of us[14,15]. However, our system is jointless from the recording place to the photodetector. Thus, the light transmission efficiency of the excitation blue light of our single fiber system is theoretically higher than compared to the ferrule systems already published that include one joint. Recently, some groups have published multi-fiber photometry systems[16,17]. These systems use bundled fibers. Bundling very thin fibers provides better spatial resolution than our single fiber system. Sometimes it seems that the activity of individual cells can be recorded. However, since the fiber is very thin, it is expected that the detection capability of changes in fluorescence is low.

Stress processing in the brain can be described as being dictated by two components. The first is a sensory discriminative component defined by strength of pain and perception of places, and the other is an emotional component that is defined by negative emotions that accompany pain such as anxiety, fear, and aversion[18,19]. Between these components, the emotional component is likely the main contributor to psychiatric disorders resulting from chronic stress because the symptom may occur long after the original sensory inputs are gone.

The neural mechanisms behind the emotional component of stress have not yet been fully elucidated. One of the reasons for this is that many stress studies utilized an acute stress paradigm in which one cannot distinguish between emotional and sensory components. These include restraint stress[20,21], intruder stress[22,23], aversive odor stress[24], auditory stress[12,25], and trembling stress[23,25]. Therefore, we do not know at present whether the above-mentioned possible contribution of orexin neurons to stress processing is within the branch of the emotional component or downstream of the sensory component.

In order to separate the components, memory-based Pavlovian testing is of interest because this method gives psychological stress to the animals after cessation of original sensory inputs. Examples are fear-conditioning from social defeat[26], electric shock[27], and mate vocalization[28]. It is interesting to point out that previous research showed that orexin neurons contribute more preferentially to psychological stressors than to physical stressors[29].

In order to clarify the activity of orexin neurons at the moment stress applied and to reveal possible relationship between orexin neuronal activity and the heart rate response, we measured orexin neuronal activity induced by aversive stress using a dual channel fiber photometry system and heart rate using a telemetry system in freely moving mice. Furthermore, we attempted to clarify the possible effect of the negative emotional component of stress in the absence of the original sensory input on orexin neuronal activity using a fear-conditioning paradigm.

Results

Setup of dual-channel in vivo fiber photometry system

Fiber photometry systems can track the real-time dynamics of genetically specified neuronal populations in the deep brain of freely moving mice by using a single fiber and genetically encoded Ca^{2+} indicators[9]. We improved this system by adding a second channel in order to be able to simultaneously detect both G-CaMP6 and mCherry. To specifically express G-CaMP6 and mCherry in orexin neurons, we prepared transgenic mice and AAV vectors as shown in Fig. 1A. The AAV mixture consisting of AAVdj-TetO-G-CaMP6 and AAVdj-TetO-mCherry was stereotaxically injected into the hypothalamus of ORX-tTA mice that express tetracycline transactivator (tTA) in orexin neurons (Fig. 1A). These AAVs can drive expression of G-CaMP6 and mCherry proteins in the presence of tTA. Three weeks after this mixture was injected, G-CaMP6 and mCherry expressed almost exclusively in hypothalamic orexin neurons (Fig. 1B). In 393 ± 60 orexin positive neurons (n = 6 animals), G-CaMP6(+) cells were 283 ± 46, mCherry(+) cells were 345 ± 59, and both G-CaMP6- and mCherry-expressing orexin neurons were 260 ± 43 (Fig. 1Bv). There was small number of ectopic expressions of G-CaMP6 (G-CaMP6(+) & orexin (-) in total G-CaMP6(+) was 8.3 %). Blue and yellow excitation lights for G-CaMP6 and mCherry were supplied by LEDs and delivered through a single optical silica fiber (Fig. 1C). Fluorescence emission from G-CaMP6 and mCherry expression in the hypothalamic orexin neurons pass back through the single optical silica fiber. The fluorescent signals pass through two dichroic mirrors and separate into green fluorescence derived from G-CaMP6 and red fluorescence derived from mCherry. The signals then arrive at their respective photomultipliers (Fig. 1C). To place the optical single silica fiber in the desired region of the hypothalamus, we implanted a guide cannula with dental cement (Fig. 1C). The guide cannula allowed the optical fiber to be placed just dorsal to the hypothalamic area of interest (Fig. 1D). The single optical silica fiber and guide cannula were made in our laboratory with the support of LUCIR Inc. (Tsukuba, Ibaraki, Japan) (Fig. 1E). These tools allowed us to obtain a stable, noiseless, and high-resolution signal. To measure electrocardiogram (ECG) and body temperature, we implanted a telemetry system transmitter (DSI) into the abdominal cavity at the same time as the guide cannula implantation (Fig. 1C). The complete system is shown in Fig. 1F. This system allowed for several types of physiological data to be measured in freely moving mice receiving food and water ad libitum. The data was measured simultaneously under a high temporal resolution (Fig. 1G). G-CaMP6 signals responded independently from shifts in mCherry signals, so we could determine whether the G-CaMP signal was real by comparing it to the levels of mCherry fluorescence. The results shown in Fig. 1 demonstrate we were able to utilize a dual channel fiber photometry system.

Association between orexin neuronal activity and aversive stress-induced autonomic responses

In order to plot real-time orexin neural activity dynamics and autonomic response dynamics before and after various types of aversive stress, we simultaneously measured G-CaMP6 fluorescence and ECG and heart rate was calculated from the ECG recordings. As an autonomic response to emotional stress, we analyzed heart rate response because change in body temperature was slow when compared to change in heart rate (see Fig. 1G). Three different stress paradigms with different sensory modalities and different afferent pathways were used. The paradigms were intruder stress, aversive sound stress, and aversive smell stress (Fig. 2A).

All of the stimuli tested, namely intruder (Fig. 2B), ultrasound (Fig. 2C), and predator odor (Fig. 2D), induced abrupt increases in heart rate (Fig. 2B-D, left column) and G-CaMP6 fluorescence (Fig. 2B-D, middle column), while mCherry fluorescence (Fig. 2B-D, right column) did not change. As the control of stress stimuli, the physiological response was measured using a cotton swab without odor and an empty box without intruders (Fig. 2E). These control stimuli did not increase GCaMP fluorescence or heart rate as much as ultrasound stress (Fig. 2F).

Although increases in G-CaMP6 fluorescence and heart rate appeared to occur simultaneously (Fig. 2B-D), closer examination revealed that there were differences in the responses. To examine possible differences in the time course, we defined onset as the time when the signal more than doubled the standard deviation of the baseline fluctuation (Fig. 3A). We then calculated Δtime to be the difference between the onset of the increase in heart rate and onset of the increase in G-CaMP6 signal. As a result, Δtime was a positive value in all the stimuli in every mouse (Fig. 3B) meaning that the change in orexin neural activity preceded the increases in heart rate in all events. It is of interest to point out that Δtime in the TMT test was significantly longer than in the intruder test and in the ultrasound test while there was no difference between the intruder test and the ultrasound test, indicating non-uniform changes in heart rate depending on stress stimuli.

We also calculated slope of the signal increase (maximum value – baseline value / time at maximum – time at the onset). This analysis revealed that slope of G-CaMP6 fluorescence change in the TMT group was significantly smaller than that in the intruder and ultrasound groups (Fig. 3C). Meanwhile, the slope of the heart rate change did not differ among the three stimuli (Fig. 3D). For TMT stimulation, activation of orexin neurons was relatively gradual when compared to the other stimulation types, and the start of the heart rate response was delayed, but the increase in heart rate ended up being similar.

Conditioned neutral sound stimulation activated orexin neurons

Although we have shown through the previous result that activation of orexin neurons precedes heart rate increase thus indicating close association between orexin neuronal activity and autonomic outcome, those experiments did not separate between the sensory component and the negative emotional component of the stressors. Subsequently, we evaluated the change in orexinergic neuronal activity resulting from exposure to a neutral tone that was previously conditioned as a cue for an unpleasant experience. With this classical conditioning paradigm, it is possible to examine the effects of the pure emotional component because the aversive electrical sensory input was no longer present at the time of testing.

First, while recording the orexin neural activity and electrocardiogram, we gave a neutral tone without electrical stimulation to the mouse (Fig. 4A Pre). No significant changes in orexin neural activity and heart rate were observed after the sound exposure (Fig. 4B left and Fig. 4C). After conditioning was established as in the protocol shown in Fig. 4A, the mouse was exposed to the sound stimulation that is identical to that was applied in the preconditioning period (Fig. 4A Post). As a result, orexin neuronal activity and heart rate increased immediately and markedly (Fig. 4B right and Fig. 4C). Furthermore, we calculated sound-induced changes in heart rate and orexin neuronal activity and compared them between before and after the conditioning (Fig. 4D). The rate of increase in heart rate and orexin neural activity were significantly increased by fear conditioning. Conversely, orexin neuronal activity and heart rate did not change (Fig. 4F, G) when exposed to the neutral tone in un-conditioning protocol shown in Fig. 4E. We examined whether conditioning was established by measuring freezing time during the observation period. As expected, conditioned group animals spent ~50% of the time in freezing while control animals did not (Fig. 4H).

Discussion

In this study, we examined whether aversive emotion has an effect on the activity of hypothalamic orexin neurons in freely moving mice. We first constructed the recording system to assess neuronal activity from the specific cell type of interest deep in the brain of freely moving mice. Using in vivo recording of hypothalamic orexin neuronal activity and ECG, we showed that every examined stress type activated orexin neurons just before the change in heart rate took place indicating a possible causative relationship between orexinergic neuronal activity and the resultant autonomic outflow. In addition, we showed that the emotional component of stress also activated orexin neurons, although the magnitude of orexin neuronal activation seems smaller than when aversive stimulation with sensory input was given. We propose that both the sensory and emotional components of stress activate orexin neurons and hence induce autonomic activation. Activation of orexin neurons when actual sensory component is absent (conditioned situation) indicates a possible contribution of the orexin system in the etiology of psychiatric disorders resulting from chronic stress because symptoms may occur after the original sensory inputs no longer occur.

The dual-channel fiber photometry system produces good signal even in freely moving mice

Using our system, we were able to record and analyze neuronal activity and autonomic responses in freely moving animals with high temporal resolution (Fig. 1G). Two-color simultaneous recording allowed us to distinguish between signal and noise with confidence. Neuronal activity recording with head-fixed mice[11,12] is an easy way to distinguish signal from noise because the animals' head is unable to move and affect the signal, but more natural behaviors cannot be measured. As a solution, measurements are taken via optical fiber from freely moving mice. However, in this case, the fiber may twist or move and the transmission efficiency at the connection between the fiber and the fluorescence detection device changes and large amounts of noise may occur. The device shown in Fig. 1 was able to eliminate these kinds of noise issues. The fluorescence ratio of green and red may also be used when analyzing data, similar to ratiometry analysis employed when using a FRET system. However, we did not calculate the ratio and instead used the red signal as an indicator of stable recording. Although we were able to exclude unstable data that occurred during large or sudden animal movements as judged by mCherry signal, it is necessary to determine a

method to completely eliminate instability in future experiments. Fiber photometry systems also often struggle with the weakness of their signals. In previous papers, authors have tried to efficiently extract fluorescent signals with various methods such as time-correlated counting system, lock-in amplifier, averaging, and ratiometric measurement[8,9,30,31]. We were able to solve this issue by implanting only a single fiber from the fluorescence detection device into the brain (Fig. 1E). Systems that use standard ferrules will commonly lose some fluorescence signals in their connections. The absence of such a joint is an advantageous feature of our system manufactured by LUCIR Inc.

Orexin neuronal activity and heart rate rapidly increase due to aversive stress stimulation irrespective of sensory modality

We showed here that orexin neuronal activity and heart rate are increased instantaneously by aversive stress in freely moving mice. Giardino et al. already showed predator odor-induced activation of the lateral hypothalamic orexin neurons using fiber photometry method[32]. Unfortunately, however, they did not assess possible autonomic consequence of the orexinergic activation. We simultaneously recorded heart rate and tried three kinds of stressors to induce aversive emotion and mice showed similar responses to each stimulus (Fig. 2). It has already been shown that heart rate increase due to intruder stress is severely attenuated in orexin deficient mice[3,4]. Therefore, orexin may be involved in the regulation of stress-induced autonomic responses. Furthermore, orexin neurons have dense innervation from the bed nucleus of the stria terminals (BNST) and the central nucleus of the amygdala (CeA)[33]. A recent study revealed that optogenetic/chemogenetic activation of GABAergic neurons in the BNST induces a rapid transition from NREM sleep to wakefulness through inactivation of melanin-concentrating-hormone neurons (which are located in the same hypothalamic region as orexin neurons[33]) and activation of orexin neurons[34]. A previous study has also shown that stress-induced autonomic responses are attenuated by pharmacological suppression of the activity of the BNST and CeA in wild type mice[6]. The central medial nucleus of the amygdala (CeM) and BNST are known as areas that regulate emotion-related autonomic responses[35]. Therefore, it is suggested that when emotional stress is given to mice, the activity of the CeM and BNST is enhanced, the orexin neurons are subsequently activated, and the autonomic response will occur[2,36]. Actually, corticotropin-releasing factor expressing BNST neurons seem to be directly connected to orexin neurons, although their connections were primarily inhibitory and suggesting complex nature of stress-induced orexinergic activation[32]. In this study, we showed that orexin neurons are promptly activated at the time of stress just preceding an increase in heart rate, thus strengthening the "emotional stress circuit" hypothesis.

Three types of aversive stress were chosen for this study because we hypothesized that if the sensory component of stress directly activates orexin neurons, there might be a different response depending on the sensory modality. However, as shown in Fig. 2, all three stress types activated orexin neurons in a similar manner even though the heart rate response from the TMT test was slightly different from that in the intruder test and ultrasonic test. Therefore, activation of orexin neurons seemed to take place after the sensory inputs of different modalities were integrated as being aversive.

Possible causal relationship between orexin neuronal activity and heart rate increase

When focusing on the differences between the starting point of the orexin neuronal activity increase and the starting point of the heart rate increase, we found that the onset of the increase in orexin neuronal activity always preceded changes in heart rate (Fig. 3B). Due to this finding, it seemed reasonable to conclude that there might be a causal relationship between them, namely that orexin neuronal activity may directly cause an increase in heart rate. Unfortunately, our data did not fully prove causality. It is necessary to directly manipulate neuronal activity, with optogenetics or pharmacogenetics for example, to conclusively prove it. Nevertheless, our data strongly support the possibility.

Differences in orexin neuronal activity depending on the type of stress stimulation

Interestingly, as shown in Fig. 3B, the Δtime is only high in the group exposed to TMT. We further examined the difference in the rate of signal rise between the three types of stressors by examining the G-CaMP6 slope. This examination shows that the G-CaMP6 fluorescence intensity increase in the TMT group is relatively moderate, that is, the neuronal activity seems to rise slowly (Fig. 3C). However, the slope of the heart rate increase in the TMT group is the same as that in the other groups (Fig. 3D). Due to these findings, we hypothesized that orexin neuronal activity needs to reach a threshold in order to increase heart rate. Taken together, the Δtime in G-CaMP6 slope was prolonged because the TMT group took longer than the other groups to reach the orexin neuronal activity threshold required to initiate heart rate increase. We do not currently have an explanation for the reasons behind why the orexin neuronal activity rises slowly only in the TMT group. It may be that because olfactory information differs from visual and auditory information in that it takes longer for the chemical substance to diffuse and bind to the receptor, and that the experimental result reflects the time difference from when the TMT stress is given until the mouse processes and interprets the odorous substances.

The negative emotional component of stress activates orexin neurons and increases heart rate

Sensory input usually increases vigilance levels in animals regardless of the valence of emotion. The orexin neuronal activity we observed (Fig. 2) may be due to an increase in awareness that accompanies an increase in attention. We were unable to distinguish whether the result of the stress-induced increases in orexin neuronal activity and the subsequent autonomic responses shown in Fig. 2 were caused by an increased vigilance caused by sensory input alone or by an "emotional change" accompanying the sensory input. Therefore, we performed an experiment to distinguish between them by utilizing a fear-conditioning paradigm. Observation of freezing behavior clearly showed that the neutral sound did not cause any aversive emotional changes unless the sound was associated with electric shock (Fig. 4B). We observed an immediate increase in orexin neuronal activity and heart rate response only when the neutral tone was previously associated with aversive emotion (Fig. 4C). This observation is in line with reports showing a possible relationship between orexin and fear behaviors[37,38]. Considering the results of Fig. 4 and the description in the previous discussion, it is possible that the changes in orexin neuronal activity observed in Fig. 2 might depend on changes in the emotion of the animals, and not the individual sensory stimulation itself.

Orexin aversive emotion response theory

In our previous study[11], we showed that orexin neurons were activated by painful stimuli (nociceptive stimuli). At that time, it was not possible to distinguish whether the response was caused by the ascending pathway from the nociceptive receptors or if it was caused by the descending pathway after the brain recognized the signal as a painful one. Although direct comparison was difficult, we now speculate that activation of orexin neurons via noxious stimulation in response to the aversive emotion that occurs in response to painful sensations was made similarly to the present study. This speculation is supported by the observation that the orexin neuronal response to noxious stimuli was eliminated under anesthesia[11].

Conclusions

This paper shows that use of LUCIR's fiber photometry system with our modification will give us a reliable signal even when the animal is actively behaving. This system can easily be used in combination with ECG, EEG, EMG recording and video tracking. It can provide simultaneous monitoring and analysis at a high temporal resolution of all the physiological pieces of information analyzed from neuronal activity deep in the brain. Although the relationship between stress and orexin neurons has been suggested, it was found that orexin neuronal activity is indeed increased due to aversive stress induced by the sensory modalities tested so far. The most important finding is that activation of orexin neurons was caused not by sensory inputs from stress but by changes in emotion to drive autonomic outputs. Aversive emotion serves a very important function as a warning system for keeping animals informed of a variety of dangers. Unfortunately, in many cases of modern society, repeated exposure to acute stress in unavoidable. For example, office workers may repeatedly suffer from aversive emotions, which may manifest in illnesses such as depression. While it may be difficult to completely escape from the stressor in these types of situations, it would be beneficial to be able to reduce the severity of the aversive emotional component. These data suggest that targeting orexin neurons may enable treatment of psychiatric disorders that result from repeated acute stress.

Methods

Animals

We used transgenic mice carrying a tetracycline-controlled transactivator transgene (tTA) under the control of the orexin promoter[11] (orexin-tTA mice, n = 45). All experimental procedures were performed in accordance with the guiding principles for the care and use of animals in the field of physiological sciences published by the Physiological Society of Japan and were approved by the Institutional Animal Use Committee at Kagoshima University (MD15075, MD17090, MD18081). Mice were maintained under a strict 12-hour light/dark cycle (light period: 7:00–19:00; dark period: 19:00–7:00) in a temperature-controlled room (22 °C). Food and water were available ad libitum and all efforts were made to minimize animal suffering and discomfort and to reduce the number of animals used.

In vivo recordings of neuronal activity using fiber photometry system and cardiovascular parameters using the radio-telemetry system

Stereotaxic AAV injection

Surgeries for AAV injections were conducted under isoflurane anesthesia (2%, inhalation) using a stereotaxic instrument (ST-7, NARISHIGE, Tokyo, Japan). A viral mixture consisting of recombinant AAV-TetO(3G)-G-CaMP6 (serotype: DJ; 600 nl/injection, $3x10^{12}$ copies/ml) and AAV-TetO(3G)-mCherry (serotype: DJ; 600 nl/injection, $6x10^{12}$ copies/ml) was stereotaxically injected into the right side the hypothalamic perifornical area (PeF) in orexin-tTA mice (Fig. 1A). The AAV mixture was injected via an air-pressure injection system (I-200J, NARISHIGE, Tokyo, Japan) connected by polyethylene tube to a glass micropipette that was made from a pulled glass tube (φ1.5 mm, World Precision Instruments, FL, USA) by a puller (Sutter Instrument Novato, CA, USA) and had a tip diameter of 18-22 μm. Injection sites was as follows: from bregma anterior 1.5 mm, lateral 0.8 mm, ventral 5.0 mm from dura.

Implantation of optical fiber for fiber photometry system

Over 2 weeks after viral injection, mice were surgically implanted with a guide cannula (LUCIR, Tsukuba, Japan) for placing the optical fiber just above the PeF to record orexin neuronal activity (Fig. 1D). At the start of the surgical procedures, mice were anesthetized with isoflurane (2–3%, inhalation), and placed on a small animal stereotaxic instrument as described previously. The site of implantation for the guide cannula was as follows: from bregma anterior 1.5 mm, lateral 0.8 mm, ventral 5.0 mm from dura. During implantation, fluorescence signal was continuously monitored so that optimal position of the fiber tip was easily recognized by abrupt increase of the output signal. The guide cannula was fixed by dental cement (Fuji LUTE BC, GC, Tokyo, Japan), gel type quick drying glue (LOCTITE 454, Henkel Japan, Yokohama, Japan), and a small anchor screw. After fixation of the guide cannula, measuring fiber was removed and a dummy cannula was inserted to prevent dust from entering the implanted guide cannula during the recovery period.

Implantation of the transducer for the radio-telemetry system

Immediately after performing the guide cannula implantation, an additional implantation surgery was performed on the mice. To measure heart rate and body temperature, we used a radio-telemetry system (Data Sciences International, St. Paul, MN, USA)(DSI). This system consists of a radio-frequency transducer (TA11PA-C20) and a receiver (RLA1020). The negative electrode (-) of the transducer was stitched into the right side of the mouse's chest cavity, the positive electrode (+) was stitched into the left side of the abdomen, and the body of the transducer was implanted into the abdominal cavity. A temperature sensor in the body of the transmitter allowed abdominal temperature to also be measured. During all surgeries, care was taken to maintain body temperature. After surgeries, mice were treated with penicillin and an analgesic, buprenorphine. For recovery, mice were individually housed and monitored and had access to food and water ad libitum for at least 1 week.

Recording

The recording was started once mice completely recovered from all surgeries and a normal circadian rhythm was present. After the recovery period, the dummy cannula was removed, an optical silica fiber (Fig. 1E) was inserted, and mice were moved to their measurement cages (Fig. 1F). Locomotor activity was recorded with a passive pyroelectric infrared motion sensor (AMN 1111, Panasonic Co., Osaka, Japan) that was attached to the ceiling of the experimental cage. Mice were housed in the cage individually during the recording period. Orexin neuronal activity and heart rate were recorded for 2–3 successive days using LabChart software version 8 (ADInstruments, New South Wales, Australia) in unrestrained, freely moving, and unanesthetized conditions.

Fiber photometry device

A fiber photometry system (COME2-FTR/OPT, LUCIR, Tsukuba, Japan) was used to record the activity of orexin neurons in freely moving mice (Fig. 1C). The system utilizes a single silica fiber that can deliver two excitation lights and detect fluorescence from G-CaMP6 and mCherry simultaneously. Blue excitation light for G-CaMP6 (470 nm, 0.5 mW at the tip of the silica fiber) and yellow excitation light for mCherry (590 nm) were produced by a high-power LED system, blue; Tholab OPT/LED Blue_TT_FC, yellow; Tholab OPT/LED yellow_TT_FC (ThoLab Japan, Tokyo, Japan). Blue and yellow excitation light was reflected by a dichroic mirror, passed through an excitation bandpass filter, and was delivered via a 400 μm silica fiber into the brain. G-CaMP6 and mCherry fluorescence were collected by the same silica fiber and guided to an individual photomultiplier for either G-CaMP6 or mCherry (PMTH-S1M1-CR131, Zolix instruments, Beijing, China) (Fig. 1F). The signal was digitized using a data acquisition system (PowerLab16/35, ADInstruments, New South Wales, Australia), and recorded by LabChart software version 8. Signals were collected at a sampling frequency of 100 Hz.

Stress stimulation

Three types of stressors were applied on the following day after the basal measurement was completed (Fig. 2A). The first was a socioemotional stressor via the resident-intruder stress test. This stressor was applied by placing an age-matched wild-type mouse (intruder mouse) contained in a small polypropylene cage into the experimental cage for 2 min. The polypropylene cage is constructed so that the intruder and resident (experimental) mice are unable to physically contact, but visual, auditory, and olfactory communication is available. The second stressor was aversive sound stress. For this test, an approximately 100 dB/25 kHz ultrasonic sound was applied to the mouse via an ultrasound-emitting device (PET-AGREE, K-II enterprise, New York, USA). The device was turned on above the cage for 2 seconds. The third stressor was aversive smell stress. For the aversive smell, 2,4,5-trimethylthiazoline, (TMT, Contech Enterprise, Victoria, Canada) a constituent of fox urine and feces, a common predator odor for mice[24,39], was placed near the nose of the mouse for 2 seconds via cotton swab.

The rationale for choosing these particular types of aversive stress were carefully considered. First, intruder stress has been used in orexin knockout mice showing a possible role of orexin neurons in stress-induced autonomic responses[3]. Second, we are interested in separating the sensory component and the emotional component of stress. If the sensory component of stress directly activates orexin neurons, there might be a

different response depending on sensory modality (optic, auditory, and olfactory) because the information transmitted to the brain from the respective receptors (eyes, ears, and nose) occurs via different sensory afferent pathways.

As the control of stress stimuli, the physiological response was measured using a cotton swab without odor and an empty box without intruders (Fig. 2E).

Fear conditioning

The animal was placed in an experimental chamber and acclimatized for 2 hours and then neutral tone sound (60 dB, 1 kHz) was given for 2 sec during fiber photometry and the heart rate recording. In order to associate a neutral tone with an unpleasant experience (Fig. 4A), 1 sec electric shock was given to the hind paw of the animal 1 to 5 sec after a 2 sec neutral tone. This was repeated 15 times using a shock generator (CBX-CT) and a cycle timer (CSG-001, Muromachi Kikai, Tokyo, Japan). After a resting period of 1 hr., the identical neutral tone was given during fiber photometry and heart rate recording. During the post-recording period, freezing behavior was also measured to confirm that classical fear conditioning had been successfully established. Freezing time was visually calculated by observing videotaped animal behavior by the experimenter who is blinded to the experimental group. No electrical stimulus was given to the control animals. All the procedures were performed in one chamber. Both behavioral test (sound stimulation and fear conditioning) including baseline recording were performed between 12:00 and 18:00.

Immunohistochemistry.

Mice were deeply anesthetized with urethane (2.0 g/kg, i.p.), and transcardially perfused with 20 ml of saline containing 20 unit/ml heparin followed by 20 ml of chilled 4% paraformaldehyde (Wako Pure Chemical Industries, Ltd., Osaka, Japan) in 0.01 M PBS (pH 7.4). The brain was removed, post-fixed in 4% paraformaldehyde solution at 4 °C overnight, and subsequently immersed in PBS at 4 °C for at least 2 days. A series of 40 μm sections were obtained with a vibratome (SuperMicroSlicer Zero1; DOSAKA EM, Kyoto, Japan). For staining, coronal brain sections were immersed in blocking buffer (1% normal horse serum and 0.3% Triton-X in PBS), then incubated with an anti-orexin A goat antibody (SC-8070, Santa Cruz Biotechnology, Inc., Dallas, TX, USA) at 4 °C overnight. The sections were washed with PBS and incubated a CF647-conjugated anti-goat IgG antibody (20048, Biotium) for 2 hrs. at room temperature. These brain sections were mounted on a slide and imaged on a fluorescence microscope (BZ-9000, Keyence, Osaka, Japan). The primary and secondary antibody were diluted in blocking buffer or PBS and consisted of anti-orexin A goat antibody used at 1:200 and CF647-conjugated anti-goat IgG antibody at 1:500. We counted G-CaMP6 positive cells (green), mCherry positive cells (red), and anti-orexin A positive cells (far red) in the hypothalamic area where orexin neurons are located (-1.0 ~ -2.0 mm from bregma) using NIH ImageJ software. We calculated the relative percentage of G-CaMP6 or mCherry positive neurons in orexin neurons by using the average number of anti-orexin A positive neurons as the reference. For counting, we used one out of every four coronal brain slices in an animal.

Statistical analysis.

Statistical analyses were performed using PRISM software (GraphPad Software, La Jolla, CA, USA). Simple comparisons of the means between the two groups were performed by Student's t-test or Mann-Whitney’s nonparametric test. Multiple comparisons of the means and SEM were performed by one-way ANOVA analyses followed by Holm-Sidak's multiple comparison tests. A P value of less than 0.05 was considered significant.

Abbreviations

BNST: the bed nucleus of the stria terminals; CeA: the central nucleus of the amygdala; CeM: The central medial nucleus of the amygdala; ECG: electrocardiogram; PeF: perifornical area; TMT: 2,4,5-trimethylthiazoline; tTA: tetracycline transactivator;

Declarations

Ethics approval and consent to participate

All experimental procedures were performed in accordance with the guiding principles for the care and use of animals in the field of physiological sciences published by the Physiological Society of Japan and were approved by the Institutional Animal Use Committee at Kagoshima University (MD15075, MD17090, MD18081).

Consent for publication

Not applicable.

Availability of data and materials

The summary statistics are available within the article. The data that support the findings of this study are available from the corresponding author upon reasonable request.

Funding

This work was supported by JSPS KAKENHI Grants (17K14936 to A. Yamashita; 17K16387 to S.M.; 16H05130 to T.K.) and CREST JST (JPMJCR1656 to A. Yamanaka) in the courses during the design of the study and collection, analysis, and interpretation of data and in writing the manuscript.

Competing interests

The authors declare that they have no competing interests.

Authors’ contributions

A.Yamashita and T.K. designed the study; A.Yamashita, S.M., R.N., J.K., A.Yamanaka and T.K. conducted the study and analyzed the data; and A.Yamashita and T.K. wrote the manuscript. All authors approved the final version of the manuscript.

Acknowledgments

We thank Jordan L. Pauli for English editing and Miki Sakoda for her excellent technical assistance and all the members of the department of Physiology for their support. We also thank all the staff members of the Institute of Laboratory Animal Sciences at Kagoshima University for keeping the animals in good condition. We acknowledge the joint research Laboratory, Kagoshima University Graduate School of Medical and Dental Sciences, for the use of their facilities.

References

1. WHO. Depression and Other Common Mental Disorders. https://www.who.int/mental_health/management/depression/prevalence_global_health_estimates/en/ (2017)
2. Kuwaki, T. Orexin links emotional stress to autonomic functions. *Auton Neurosci**161***, 20–27. http://doi.org/10.1016/j.autneu.2010.08.004 (2011).
3. Kayaba, Y., et al. Attenuated defense response and low basal blood pressure in orexin knockout mice. *Am J Physiol Regul Integr Comp Physiol**285***, R581–R593. http://doi.org/10.1152/ajpregu.00671.2002 (2003).
4. Zhang, W., Sakurai, T., Fukuda, Y. & Kuwaki, T. Orexin neuron-mediated skeletal muscle vasodilation and shift of baroreflex during defense response in mice. *Am J Physiol Regul Integr Comp Physiol**290***, R1654-R1663. http://doi.org/10.1152/ajpregu.00704.2005 (2006).
5. Mileykovskiy, B., Kiyashchenko, L. & Siegel, J. Behavioral correlates of activity in identified hypocretin/orexin neurons. *Neuron**46***, 787-798 (2005).
6. Lee, M. G., Hassani, O. K., & Jones, B. E. Discharge of identified orexin/hypocretin neurons across the sleep-waking cycle. *J Neurosci**25***, 6716–6720 http://doi.org/10.1523/JNEUROSCI.1887-05.2005 (2005).
7. Zhang, W., Zhang, N., Sakurai, T. & Kuwaki, T. Orexin neurons in the hypothalamus mediate cardiorespiratory responses induced by disinhibition of the amygdala and bed nucleus of the stria terminalis. *Brain Res**1262***, 25–37. http://doi.org/10.1016/j.brainres.2009.01.022 (2009).
8. Cui, G., et al. Deep brain optical measurements of cell type–specific neural activity in behaving mice. *Nat Protoc**9***, 1213–1228. http://doi.org/10.1038/nprot.2014.080 (2014).
9. Gunaydin, L. A., et al. Natural neural projection dynamics underlying social behavior. *Cell**157***, 1535–1551. http://doi.org/10.1016/j.cell.2014.05.017 (2014).
10. Guo, Q., et al. Multi-channel fiber photometry for population neuronal activity recording. *Biomed Opt Express**6***, 3919. http://doi.org/10.1364/BOE.6.003919 (2015).
11. Inutsuka, A., et al. The integrative role of orexin/hypocretin neurons in nociceptive perception and analgesic regulation. *Sci Rep**6***, 29480. http://doi.org/10.1038/srep29480 (2016).
12. Moriya, S., et al. Acute aversive stimuli rapidly increase the activity of ventral tegmental area dopamine neurons in awake mice. *Neurosci*, ***386***, 16–23. http://doi.org/10.1016/J.NEUROSCIENCE.2018.06.027 (2018).

13. Futatsuki, T., et al. Involvement of orexin neurons in fasting- and central adenosine-induced hypothermia. *Sci Rep* ***8***, 2717. http://doi:10.1038/s41598-018-21252-w (2018).
14. Simone, K., Füzesi, T., Rosenegger, D., Bains, J., Murari, K. Open-source, cost-effective system for low-light *in vivo* fiber photometry. *Neurophotonics*, ***5(2)***, 025006. http://doi:10.1117/1.NPh.5.2.025006. (2018).
15. Meng, C., et al. Spectrally resolved fiber photometry for multi-component analysis of brain circuits. *Neuron*, ***98(4)***, 707-717. http://doi:10.1016/j.neuron.2018.04.012. (2018).
16. Martianova E, Aronson S, Proulx CD. Multi-fiber photometry to record neural activity in freely-moving animals. *J Vis Exp.* ***152***, e60278. http://doi:10.3791/60278. (2019).
17. Sych, Y., Chernysheva, M., Sumanovski, L.T., Helmchen, F. High-density multi-fiber photometry for studying large-scale brain circuit dynamics. *Nat Methods*. ***16(6)***, 553-560. http://doi:10.1038/s41592-019-0400-4. (2019).
18. Minami, M. Neuronal mechanisms underlaying pain-induced negative emotion. *BRAIN and NERVE*, ***64***, 1241-1247. https://doi.org/10.11477/mf.1416101337 (Japanese. Abstract in English) (2012).
19. Minami, M. & Ide, S. How does pain induce negative emotion? role of the bed nucleus of the stria terminalis in pain-induced place aversion. *Curr Mol Med* ***15***, 184–190. http://doi.org/10.2174/1566524015666150303002336 (2015).
20. Sharma, H. S. Blood–Brain and Spinal Cord Barriers in Stress. In: Sharma H.S. and Westman, J (Eds) *Blood-Spinal Cord and Brain Barriers in Health and Disease*, Elsevier, pp. 231–298. http://doi.org/10.1016/B978-012639011-7/50019-X (2004).
21. Grafe, L. A., et al. Orexin 2 receptor regulation of the hypothalamic–pituitary–adrenal (HPA) response to acute and repeated stress. *Neurosci* ***348***, 313–323. http://doi.org/10.1016/j.neuroscience.2017.02.038 (2017).
22. Kurihara, Y., et al. Role of endothelin-1 in stress response in the central nervous system. *Am J Physiol Regul Integr Comp Physiol* ***279***, R515–R521. http://doi.org/10.1152/ajpregu.2000.279.2.R515 (2000).
23. Ikoma, Y., Kusumoto-Yoshida, I., Yamanaka, A., Ootsuka, Y. & Kuwaki, T. Inactivation of serotonergic neurons in the rostral medullary raphé attenuates stress-induced tachypnea and tachycardia in mice. *Front Physiol* ***9***, 832. http://doi.org/10.3389/fphys.2018.00832 (2018).
24. Hotsenpiller, G. & Williams, J. L. A synthetic predator odor (TMT) enhances conditioned analgesia and fear when paired with a benzodiazepine receptor inverse agonist (FG-7142). *Psychobiology*, ***25***, 83–88. http://doi.org/10.3758/bf03327031 (1997).
25. Iwakawa, S., Kanmura, Y. & Kuwaki, T. Orexin receptor blockade-induced sleep preserves the ability to wake in the presence of threat in mice. *Front Behav Neurosci* ***12***, 327. http://doi.org/10.3389/fnbeh.2018.00327 (2019).
26. Golden, S. A., Covington, H. E., Berton, O. & Russo, S. J. A standardized protocol for repeated social defeat stress in mice. *Nat Protoc* ***6***, 1183–1191. http://doi.org/10.1038/nprot.2011.361 (2011).
27. Furlong, T. & Carrive, P. Neurotoxic lesions centered on the perifornical hypothalamus abolish the cardiovascular and behavioral responses of conditioned fear to context but not of restraint. *Brain Res* **1128**, 107-119. http://doi.org/10.1016/j.brainres.2006.10.058 (2007).

28. Murata, Y., et al. A high fat diet-induced decrease in hippocampal newly-born neurons of male mice is exacerbated by mild psychological stress using a Communication Box. *J Affect Disord* ***209***, 209–216. http://doi.org/10.1016/J.JAD.2016.11.046 (2017).
29. Furlong, T. M., Vianna, D. M. L., Liu, L. & Carrive, P. Hypocretin/orexin contributes to the expression of some but not all forms of stress and arousal. *Eur J Neurosci* ***30***, 1603–1614. http://doi.org/10.1111/j.1460-9568.2009.06952.x (2009).
30. Isosaka, T., et al. Htr2a-expressing cells in the central amygdala control the hierarchy between innate and learned fear. *Cell*, ***163***, 1153–1164. http://doi.org/10.1016/J.CELL.2015.10.047 (2015).
31. Natsubori, A., et al. Ventrolateral striatal medium spiny neurons positively regulate food-incentive, goal-directed behavior independently of D1 and D2 selectivity. *J Neurosci* ***37***, 2723–2733 (2017). http://doi.org/10.1523/JNEUROSCI.3377-16.2017
32. Giardino, W.J, et al. Parellel circuits from the bed nuclei of stria terminalis to the lateral hypothalamus drive oppisng emotional states. *Nat Neurosci* ***21***, 1084-1095. https://doi.org/10.1038/s41593-018-0198-x (2018).
33. Sakurai, T. The role of orexin in motivated behaviours. *Nat Rev Neurosci* ***15***, 719–731. http://doi.org/10.1038/nrn3837 (2014).
34. González, J. A., Iordanidou, P., Strom, M., Adamantidis, A. & Burdakov, D. Awake dynamics and brain-wide direct inputs of hypothalamic MCH and orexin networks. *Nat Commun* ***7***, 11395. http://doi.org/10.1038/ncomms11395 (2016).
35. LeDoux, J.E., Iwata, J., Cicchetti, P. & Reis, D.J. Different projections of the central amygdaloid nucleus mediate autonomic and behavioral correlates of conditioned fear. *J Neurosci* ***8***, 2517**–**2529. https://doi.org/10.1523/JNEUROSCI.08-07-02517.1988 (1988).
36. Carrive, P. & Kuwaki, T. Orexin and Central Modulation of Cardiovascular and Respiratory Function. In Lawrence A. and de Lecea L. (Eds) *Behavioral Neuroscience of Orexin/Hypocretin. Current Topics in Behavioral Neuroscience vol 33,* Springer, pp. 157–196. http://doi.org/10.1007/7854_2016_46 (2016).
37. Flores, Á., Saravia, R., Maldonado, R. & Berrendero, F. Orexins and fear: implications for the treatment of anxiety disorders. *Trend Neurosci* ***38***, 550–559. http://doi.org/10.1016/j.tins.2015.06.005 (2015).
38. Soya, S., et al. Orexin modulates behavioral fear expression through the locus coeruleus. *Nat Commun* ***8***, 1606. http://doi.org/10.1038/s41467-017-01782-z (2017).
39. Rampin, O., et al. Where is the TMT? GC-MS analyses of fox feces and behavioral responses of rats to fear-inducing odors. *Chem Senses*, ***43***, 105–115. http://doi.org/10.1093/chemse/bjx075 (2018).

Figures

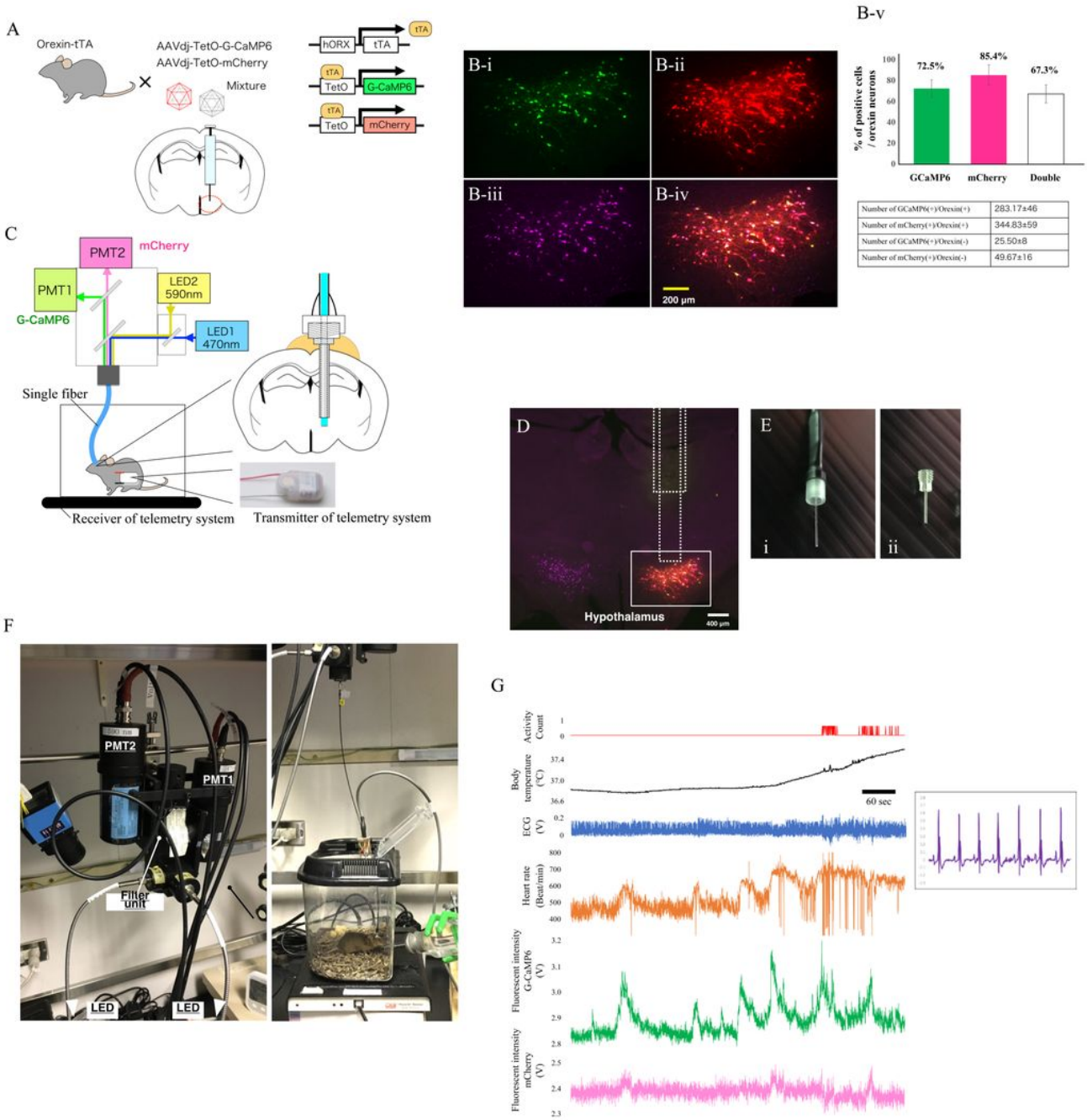

Figure 1

Simultaneous real time measurement of orexin neural activity, heart rate, and body temperature in freely moving mice using a fiber photometry and telemetry system. (A) Schematic drawing showing specific expression of G-CaMP6 and mCherry in orexin neurons by injecting AAV vectors into the hypothalamus of Orexin-tTA transgenic mice. (B) Immunohistochemical confirmation showing G-CaMP6 (B-i) and mCherry (B-ii) were exclusively expressed in almost all orexin neurons (B-iii) that were visualized by anti Orexin A-antibody in Orexin-tTA mice. G-CaMP6 and mCherry identified by their own fluorescence. Scale bar is 50 μm.

Images are close-up of the white rectangle in D. B-v) Quantification of G-CaMP-positive cells, mCherry-positive cells, and G-AcMP6 and mCherry double positive cells in hypothalamic orexin neurons. (C) Schematic diagram of dual channel fiber photometry system. Blue excitation light from the 470 nm LED illuminates the G-CaMP6-expressing neurons in the hypothalamus via optical fiber. Green fluorescence from G-CaMP6 is then gathered by the same optical fiber and detected by the photomultiplier tube (PMT). Body temperature and heart rate were measured by a telemetry system. Telemetry transmitter was intraperitoneally implanted into the mouse. (D) Confirmation of the fiber tract after fluorescent recordings. Coronal section of the brain from the orexin-tTA mouse injected with AAV-TetO(3G) G-CaMP6 and AAV-TetO(3G) mCherry mixture 2 weeks before recording. The dashed line indicates the location of the inserted guide cannula and optic fiber. The white square indicates the hypothalamus region. (E) Self-assembled silica connecting cable called the “patch cord” (i) and in vivo optical fiber cannula (ii). (F) Overall fiber photometry system. (G) Representative traces of locomotor activity (activity count), body temperature, electrocardiography (ECG, expanded traces in the rectangle), heart rate (calculated as beats per minute), and the fluorescence intensity of G-CaMP6 and mCherry in the orexin neurons.

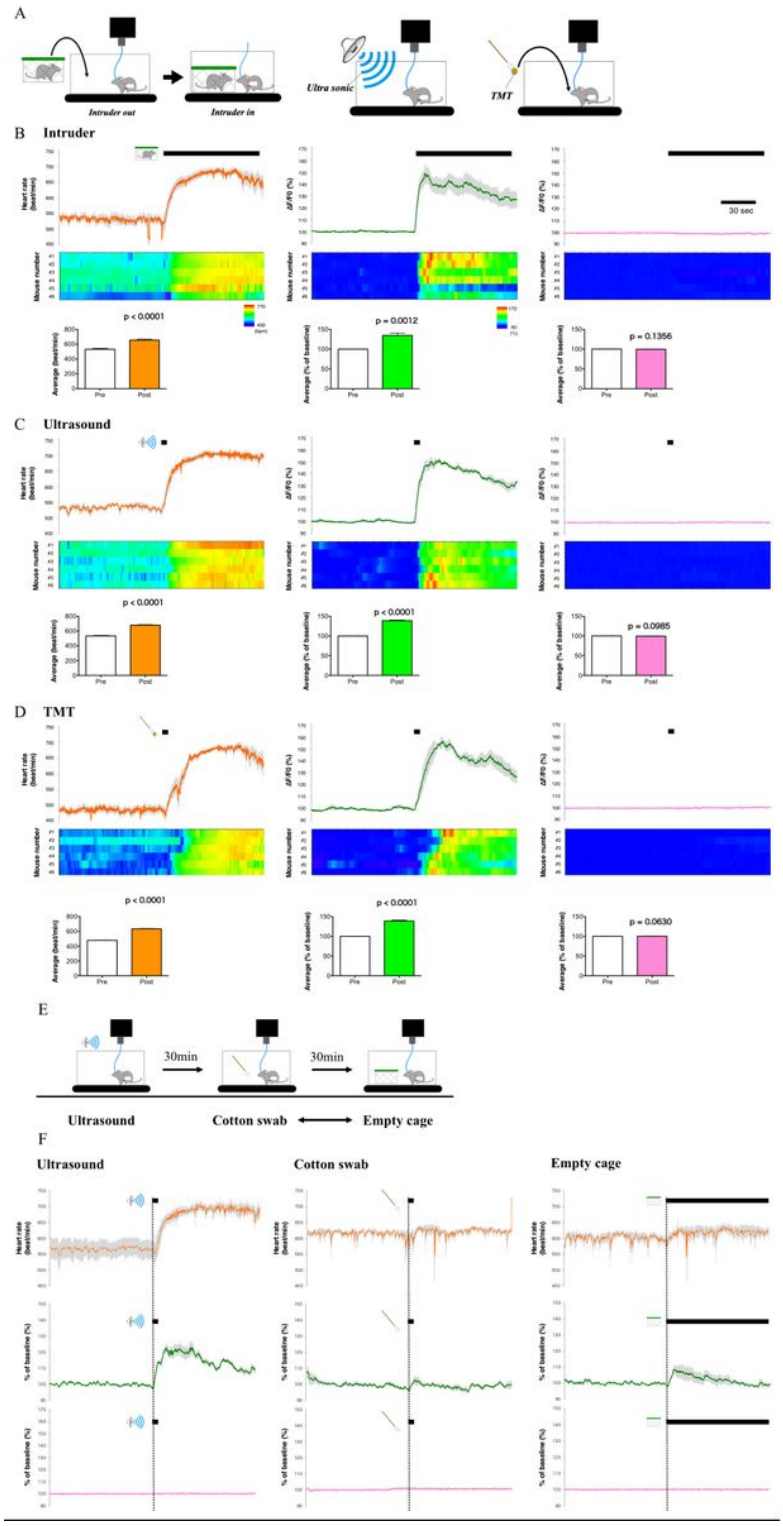

Figure 2

Aversive stress activated orexin neurons together with an increase in heart rate. (A) Schematic drawing showing the experimental design; intruder stress (left), ultrasound stress (middle), and predator odor (TMT) stress (right). (B) Results of intruder stress experiment. The horizontal bar shows the time when the intruder was in the experimental chamber for 2 min. i) (upper) Averaged time course of the heart rate during the intruder test. Mean value is shown in the orange line and SEM is shown in gray. (middle) Heat maps show the heart rate in individual animals. (lower) Bar graph shows averaged values of the heart rate for 1min

during the baseline period and after introduction of an intruder. ii) (upper) Averaged time course of the G-CaMP6 fluorescence during intruder test. Mean value is shown in the green line and SEM is shown in gray. Horizontal bar shows the time when intruder was in the experimental chamber. (middle) Heat maps show G-CaMP6 fluorescence in individual animals. (lower) Bar graph shows averaged values of the intensity of G-CaMP6 fluorescence for 1 min during the baseline period and after introduction of intruder. iii) Results of mCherry fluorescence are shown in a similar manner to B-ii. (C) Results of the ultrasound stress experiment. Data are shown in a similar manner to B. The horizontal bar shows the time when ultrasound was applied for 2 sec. (D) Results of TMT smell experiment. Data are shown in a similar manner to B. The horizontal bar shows the time when TMT was applied for 2 sec. Data were sampled in 6 animals in intruder test and ultrasound stimulation and 7 animals in TMT test. Group data are presented as mean ± SEM. P value was calculated using paired student's t-test. (E) Schematic drawing showing the control experimental design; mice (n=4) were given ultrasound stress for positive control. Then odorless cotton swab and empty cage were presented in interval of 30 min. For randomization, 2 mice received cotton swab for the first time and the other mice received empty cage for the first time. (F) Traces of the heart rate (upper), G-CaMP6 fluorescence (middle), and fluorescence of mCherry (lower) in ultrasound stress group (left), cotton swab group (middle) and empty cage group (right). The colored line indicates averaged value and the gray line shows SEM.

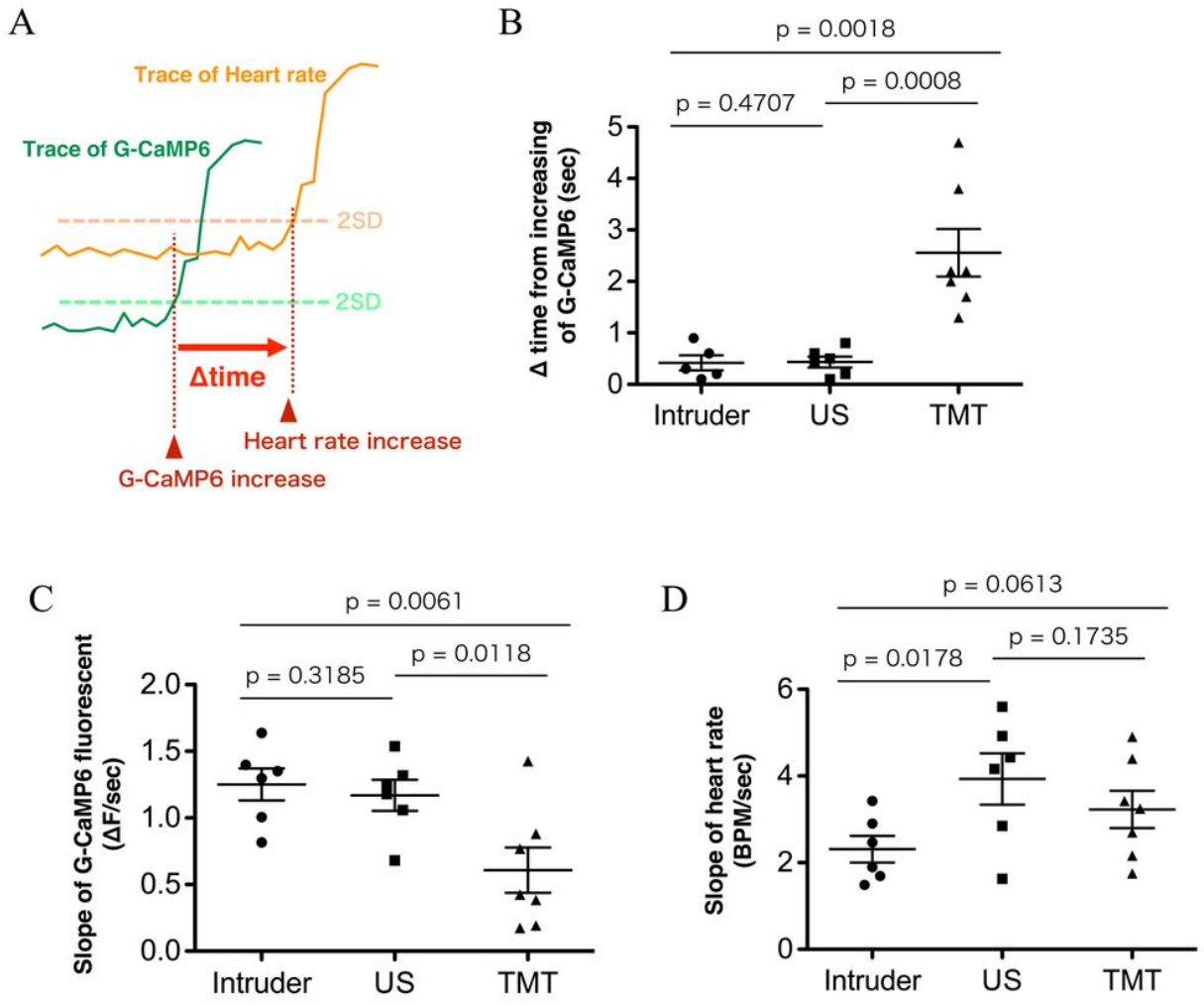

Figure 3

Comparison of onset latencies and increasing rate between the change in G-CaMP6 fluorescence and those in the heart rate (A) Schematic drawing of the definition of Δtime. Δtime was defined as the difference between the onset of fluorescence change and the onset of heart rate change. Onset was defined as the time when the signals first exceeded 2SD from the baseline fluctuation. (B) Plots of Δtime in the three stress experiments (intruder, ultrasonic sound; US, and TMT). Horizontal bars indicate average value and SEM. One-way ANOVA indicated there was significant statistical difference among stresses ($F_{2,15} = 20.70$, $P < 0.0001$). Holm-Sidak's multiple comparison was used as post hoc test (P values in the figure). (C) Plots of the slope in G-CaMP6 fluorescence. Slope of the signal increase was defined as (maximum value – baseline value / time at maximum – time at the onset). Horizontal bars indicate average value and SEM. One-way ANOVA indicated there was statistical difference between stresses ($F_{2,15} = 4.851$, $P = 0.0237$). Holm-Sidak's multiple comparison was used as post hoc test (P values in the figure). (D) Plots of the slope in heart rate trace. Horizontal bars indicate average value and SEM. One-way ANOVA indicated there was no statistical difference among stresses ($F_{2,15} = 3.094$, $P = 0.075$). Holm-Sidak's multiple comparison was used as post hoc test (P values in the figure). Data were sampled in 6 animals.

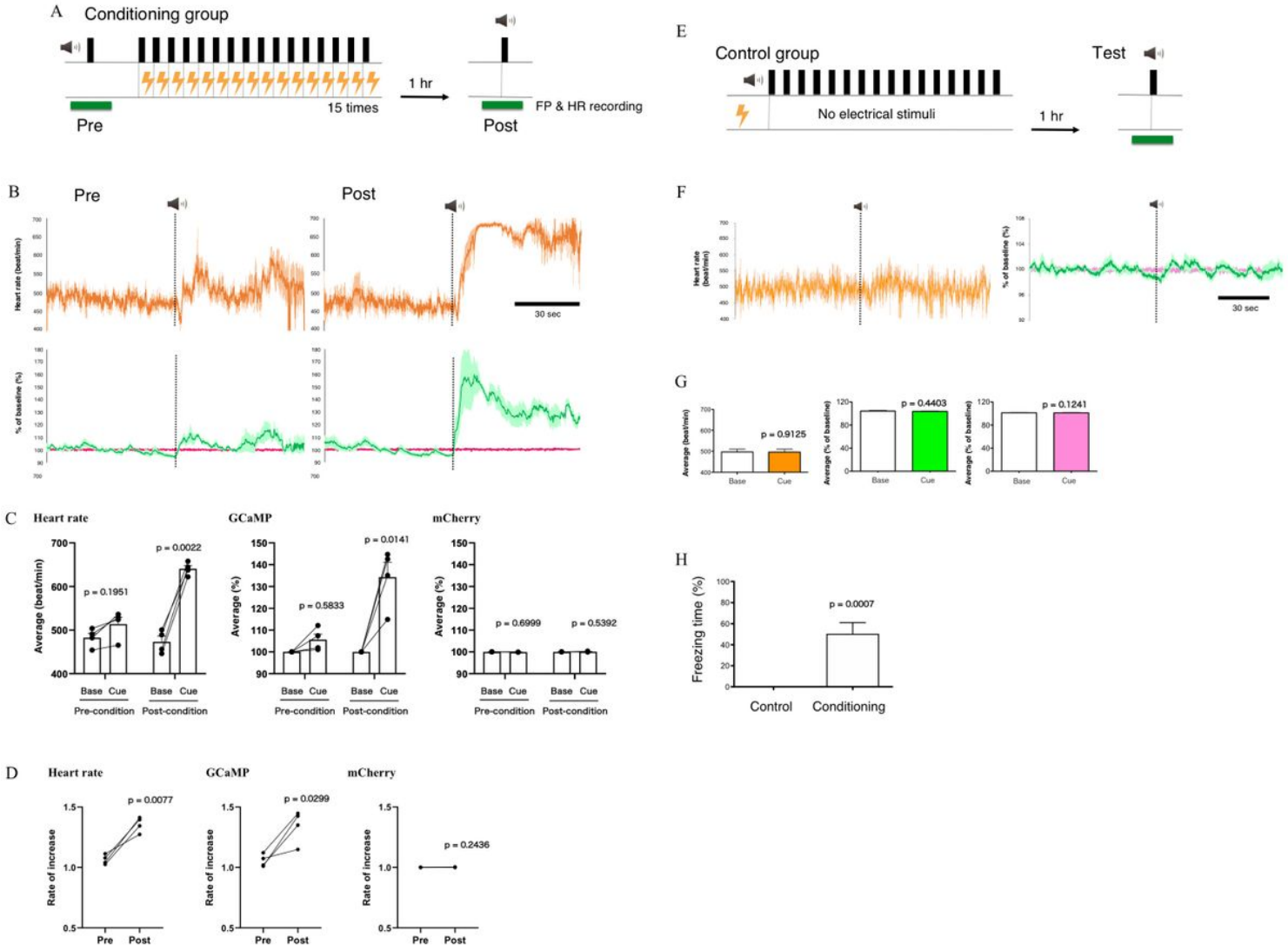

Figure 4

Conditioning-induced activation of orexin neuron and increase in heart rate without aversive sensory input (A) Experimental design for neuronal and heart rate recordings of conditioning group (n = 4). HR and fluorescence were recorded for 2 min around sound application before conditioning (pre) and 1hr after conditioning (post). HR and fluorescence were averaged for 1 min during the baseline period and after the cue sound (green horizontal line). (B) Traces of the heart rate (upper), G-CaMP6 and mCherry fluorescence (lower) in pre-conditioning (left) and post-conditioning (right) in the conditioning group. The colored line indicates the averaged value and the gray line shows SEM. (C) Grouped average and SEM of the averaged values for 1 min during the baseline period and after the cue sound. Two-way ANOVA revealed that there was significant difference between baseline and cue sound (Heart rate: F1, 3 = 8.719, P = 0.0599; G-CaNP6: F1,3 = 15.22, P = 0.0299; mCherry: F1,3 = 2.096, P = 0.2435) and between pre-condition and post-condition (Heart rate: F1, 3 = 622.9, P < 0.0001; G-CaMP6: F1,3 = 30.91, P = 0.0115; mCherry: F1,3 = 0.04808, P = 0.8405). P values in the figure were calculated by Holm-Sidak's multiple comparison test. (D) Changes in the rate of increase due to the cue sound of individual mice. The rate of increase is represented by the average of after cue sound / the average of before cue sound. P values were calculated using a paired t-test. (E) Experimental design for neuronal and heart rate recordings in the control group (n = 11). (F) Traces of the

heart rate (left), G-CaMP6 and mCherry fluorescence (right) in the control group. (G) Grouped average and SEM of the averaged values for 1 min during the baseline period and after the cue sound. P values were calculated using paired t-test. (H) Results of the freezing score (% time) during cue test tone. In the post-session, freezing behavior was counted in the control group (n = 11) and in the conditioned group (n = 4). P values was calculated using Mann-Whitney’s nonparametric test.